Particuology 11 (2013) 483–489

Contents lists available at ScienceDirect

Particuology

journal homepage: www.elsevier.com/locate/partic

Granulation by spray coating aqueous solution of ammonium sulfate to produce large spherical granules in a fluidized bed

Guanda Wang, Ling Yang, Rui Lan, Tingjie Wang*, Yong Jin

Department of Chemical Engineering, Tsinghua University, Beijing 100084, China

ARTICLE INFO

Article history:
Received 9 July 2012
Received in revised form 5 October 2012
Accepted 14 October 2012

Keywords:
Ammonium sulfate
Spray coating
Granulation
Fluidized bed
Heterogeneous crystallization

ABSTRACT

Spherical 2–4 mm granules of ammonium sulfate $(NH_4)_2SO_4$ are promising fertilizer for practical use, though only much smaller grains are being produced in industry. This work used coating granulation to produce large spherical granules of $(NH_4)_2SO_4$ in a fluidized bed by spraying its aqueous solution onto 0.9–1.6 mm $(NH_4)_2SO_4$ core particles. However, the overall coating efficiency was only 58% due to loss as dust by attrition of $(NH_4)_2SO_4$ in the vent gas. By adding $CaCO_3$ or SiO_2 particles into the feed solution, the coating efficiency was increased to over 90%. This increase in coating efficiency was due to a change in the crystallization mechanism of $(NH_4)_2SO_4$. The added $CaCO_3$ or SiO_2 particles provided a heterogeneous surface that induced $(NH_4)_2SO_4$ to crystallize uniformly to form a more compact structure less susceptible to attrition.

1. Introduction

Ammonium sulfate ($(NH_4)_2SO_4$) is an excellent fertilizer which provides nitrogen (N) and sulfur (S) nutrients to plants. Compared to nitrogenous fertilizers such as urea and NH_4NO_3, $(NH_4)_2SO_4$ gives better agronomic and environmental benefits (Chien, Gearhart, & Villagarcia, 2011), which include: (1) $(NH_4)_2SO_4$ is acidic in soil solution, so NH_3 volatilization can be prevented, while urea is easily hydrolyzed to give N loss by NH_3 volatilization, (2) $(NH_4)_2SO_4$ has positive effects on soil acidification that increases the availability of soil phosphorus (P), (3) $(NH_4)_2SO_4$ results in less NO_3^- (N) leaching, while the NO_3^- ion in NH_4NO_3 is susceptible to leaching, and (4) $(NH_4)_2SO_4$ is a S source for the soil.

$(NH_4)_2SO_4$ is mainly obtained as byproducts from caprolactam production (Tinge et al., 2007), coking processes and power plant desulfurization flue gas (Chou, Bruinius, Benig, Chou, & Carty, 2005). $(NH_4)_2SO_4$ can also be produced from the conversion of phosphogypsum, which makes use of a waste material and reduces environmental pollution (Hagiu, Ciupitu, & Apostolescu, 1998; Hanna & Ahmed, 1999). Normally $(NH_4)_2SO_4$ is produced in the form of small crystalline grains. However, for use as an agricultural fertilizer, $(NH_4)_2SO_4$ in the form of large granules of 2–4 mm in diameter is preferred for easy mixing into the bulk blended fertilizer. Also, large granules have a slower release rate (Hemati, Cherif, Saleh, & Pont, 2003).

In this work, a coating granulation method was developed by spray-coating $(NH_4)_2SO_4$ aqueous solution on core particles of $(NH_4)_2SO_4$ in a fluidized bed. An industrial byproduct of aqueous $(NH_4)_2SO_4$ solution of high concentration can be directly used as the feed solution in this granulation method to give a more economic and energy-efficient alternative to the crystallization process. In this process, core particles were introduced and fluidized in a granulator into which a $(NH_4)_2SO_4$ feed solution was atomized via a nozzle and continuously sprayed onto the core particles. As the water in the solution evaporated, $(NH_4)_2SO_4$ solute was deposited onto the surface of the core particles and the coating grew by a "layering" growth mechanism (Hemati et al., 2003). A previous study by Uemaki and Mathur (1976) investigated the mass and heat balances in the granulation of $(NH_4)_2SO_4$ fertilizer in a spouted bed using 40% $(NH_4)_2SO_4$ aqueous solution, but there has been no further report on this granulation process.

The coating efficiency, which is the proportion of the material used that contributes to the growth of the granules, is an important criterion. In an exploratory work where pure $(NH_4)_2SO_4$ aqueous solution (40 wt%) was used in the spray coating, over 40% of the solute was lost as dust, thus resulting in a low coating efficiency. A higher coating efficiency is needed for reducing material loss and energy consumption. Löffler (1988) reported that the coating efficiency is determined by droplet collection efficiency on the core particle surface and attrition losses. Our preliminary analysis using SEM images of the granule structure showed that the

* Corresponding author. Tel.: +86 10 62788993; fax: +86 10 62772051.
E-mail address: wangtj@tsinghua.edu.cn (T. Wang).

1674-2001/$ – see front matter
http://dx.doi.org/10.1016/j.partic.2012.10.005

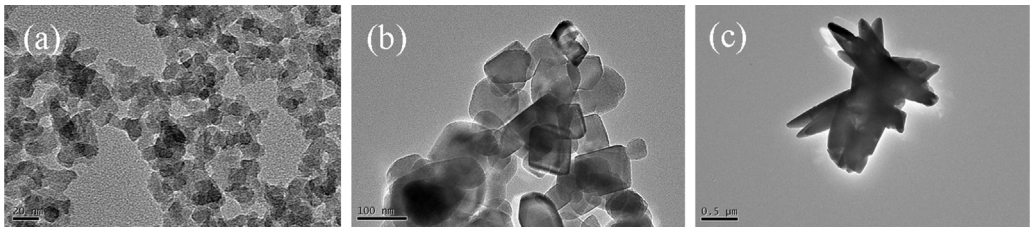

Fig. 1. TEM images of the additive particles: (a) nano-SiO_2; (b) nano-$CaCO_3$; (c) micro-$CaCO_3$.

dust formation was possibly due to attrition caused by the weak adhesion of the newly deposited solute on the granule surface. In this work, the key factors affecting coating efficiency and granule structure during the crystallization of the $(NH_4)_2SO_4$ coating were studied.

The crystallization of $(NH_4)_2SO_4$ could be changed by introducing foreign heterogeneous nuclei. Many research workers showed that fine foreign particles could induce the heterogeneous crystallization of $(NH_4)_2SO_4$. Martin, Schlenker, Holly, and Duckworth (2001) reported that mineral dust constituents such as corundum, hematite and anatase, 250–2000 nm in size, promoted the crystallization of $(NH_4)_2SO_4$ particles. Pant, Parsons, and Bertram (2006) found that 1 wt% of kaolinite induced the crystallization of $(NH_4)_2SO_4$ at low supersaturation. Onasch, McGraw, and Imre (2000) studied the crystallization of an aqueous $(NH_4)_2SO_4$ droplet containing calcium carbonate dust and showed that the $CaCO_3$ served as a catalyst for heterogeneous nucleation, causing $(NH_4)_2SO_4$ to crystallize at a higher relative humidity than in homogeneous crystallization. A similar result was reported by Oatis, Imre, McGraw, and Xu (1998), that is, the presence of $CaCO_3$ strongly affected $(NH_4)_2SO_4$ crystallization.

In this work, nano- and micro-sized $CaCO_3$ particles were added into the $(NH_4)_2SO_4$ solution as heterogeneous nuclei. Nano-sized SiO_2 particles were also used for comparison. The influences of the additive particles on coating efficiency and granule crushing strength were also investigated. The effects of the heterogeneous nuclei on $(NH_4)_2SO_4$ crystallization were analyzed.

2. Experimental

2.1. Materials and reagents

The $(NH_4)_2SO_4$ used in the experiments was a commercial product (Sinopec Baling Petrochemical Company, China). Nano-sized SiO_2 (JF555, Jianfeng Chemicals Co., Ltd., Chongqing, China), nano- and micro-sized $CaCO_3$ (Calane Ultrafine Material Co., Ltd., Beijing, China) used were also commercial products. These were used as additives dispersed into the $(NH_4)_2SO_4$ solution. The particle morphologies of the additives are shown in Fig. 1. The properties of the additives are listed in Table 1.

2.2. Granulation apparatus

A schematic diagram of the granulation apparatus is shown in Fig. 2. The spray nozzle was located at the bottom of the fluidized bed. The diameter of the distributor plate was 100 mm.

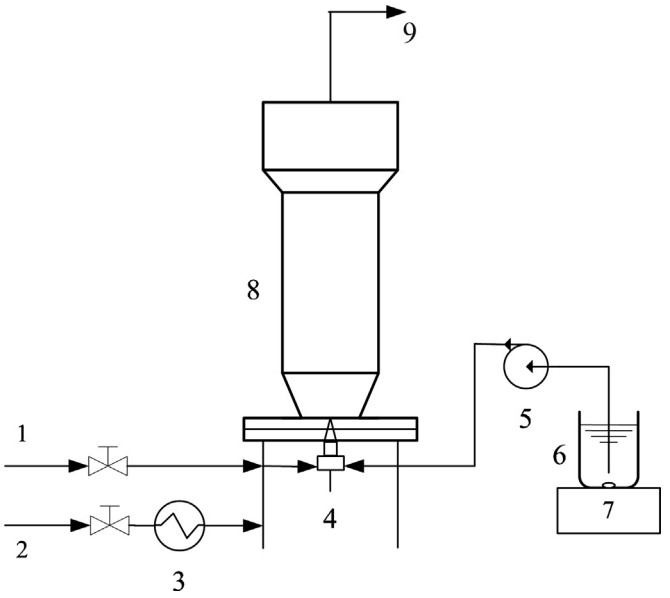

Fig. 2. The granulation apparatus. (1) Atomizing gas; (2) fluidizing gas; (3) heater; (4) nozzle; (5) peristaltic pump; (6) $(NH_4)_2SO_4$ solution vessel; (7) stirrer; (8) fluidized bed; (9) vent gas.

The bottom of the fluidized bed was cone shaped to enhance fluidization of the granules. The height of this conical section was 150 mm. The main cylinder section was 150 mm in diameter and 450 mm in height. The expanded section, 250 mm in diameter, at the top of the fluidized bed was designed to prevent the granules from being entrained. The height of this section was 200 mm. The fluidizing air was supplied by a compressor and heated by a heater. The vent gas was exhausted after dust collection. The atomizing air was supplied by another compressor. The $(NH_4)_2SO_4$ solution was pumped into the nozzle by a peristaltic pump.

2.3. Spray coating granulation

In each experiment, 1 kg crystal grains of 0.9–1.6 mm in size were sieved from the commercial $(NH_4)_2SO_4$ and used as the core particles in the granulation. 10.5 kg of 40.0 wt% $(NH_4)_2SO_4$ solution was used as the feed solution. As the granules grew up, the bed height was controlled by taking out certain amount of granules after each 1.5 kg $(NH_4)_2SO_4$ solution was sprayed.

Table 1
Additive particle parameters.

Additives	Shape	Size (nm)	Specific surface area (m^2/g)
Nano-SiO_2	Spherical-like	~20	183.677
Nano-$CaCO_3$	Cubic-like	~100	16.241
Micro-$CaCO_3$	Spindle-shape	(100–200) × (1500–2000)	2.389

Table 2
Experimental conditions.

Fluidizing air temperature (°C)	90
Spray rate (mL/min)	40
Atomizing air flow rate (m^3/h)	4
Fluidizing air flow rate (m^3/h)	100–140
$(NH_4)_2SO_4$ concentration (wt%)	40.0
Atomizing air pressure (MPa)	0.30

Each granulation experiment was divided into seven stages. In each stage, the $(NH_4)_2SO_4$ solution was prepared as follows. 600 g of $(NH_4)_2SO_4$ was dissolved in 900 g deionized water. A certain amount (1%, 2%, 3%, 4% and 5% of the amount of $(NH_4)_2SO_4$) of dried additive was weighed and added. First, a slurry was prepared by dispersing the additives into 400 mL of the aqueous solution using an electrical beater. The additive was well dispersed in the slurry after beating for 2 min. Then the slurry was mixed into the rest of the $(NH_4)_2SO_4$ solution and the mixture was stirred with an electromagnetic stirrer to keep the additives suspended in the solution. The solution was pumped into the nozzle, atomized by pressurized air, and sprayed onto the granules, and it crystallized during dewatering. The fluidizing air flow rate was adjusted from 100 to 140 m^3/h during granule growth to keep the bed fully fluidized. When each spray coating stage was completed, all the granules were taken out and weighed, and then 1 kg of the granules were returned to the fluidized bed as core particles for the next stage. By this method, the initial bed height of each stage was maintained relatively constant. The experimental conditions are listed in Table 2.

The granulation time used to produce the final granules in the experiments was about 230 min. After all seven stages were completed, the granules were kept fluidized at 90 °C for 20 min to further dewater and crystallize the granules. The samples were kept in sealed plastic bags to keep them away from the moisture in the air.

2.4. Coating efficiency calculation

The overall coating efficiency E was calculated by

$$E = \frac{W_p - W_i}{W_{as} + W_{ad}} \times 100\%, \quad (1)$$

where W_p was the total weight of the product granules obtained from all seven stages, W_i was the weight of the initial core particles (1 kg), W_{as} was the weight of the $(NH_4)_2SO_4$ (7×0.6 kg), and W_{ad} was the weight of the additive.

2.5. Granule crushing strength measurement

The crushing strength is an index used to characterize granule hardness (Walker et al., 1997). For each experiment, 200 granules were sampled from the final product. A micrometer (0–25 mm, accuracy 10 μm) was used to measure their diameters. A particle strength tester (Yinhe Instrument Factory, Jiangyan, China) was used to measure the granule crushing strength by applying an increasing compressive force on a single granule. The tester recorded the compressive force when the granule was crushed. In the fertilizer industry, the Newton is the unit used for the granule crushing strength. A scatter diagram of granule strength versus diameter was plotted from the data.

3. Results and discussion

3.1. Granules produced

The final product was spherical granules with sizes of 2–4 mm. Fig. 3(a) shows the granules produced with pure $(NH_4)_2SO_4$ and $(NH_4)_2SO_4$ with 5% micro-$CaCO_3$ additives. A scanning electron microscope (SEM, JSM7401, JEOL, Japan) was used for observing the granule morphology. By cutting single granules, the core–shell structure of the cross section is presented in Fig. 3(b), showing that $(NH_4)_2SO_4$ was coated onto the core particles, and that the structure of the coated layer in the radial direction showed no obvious

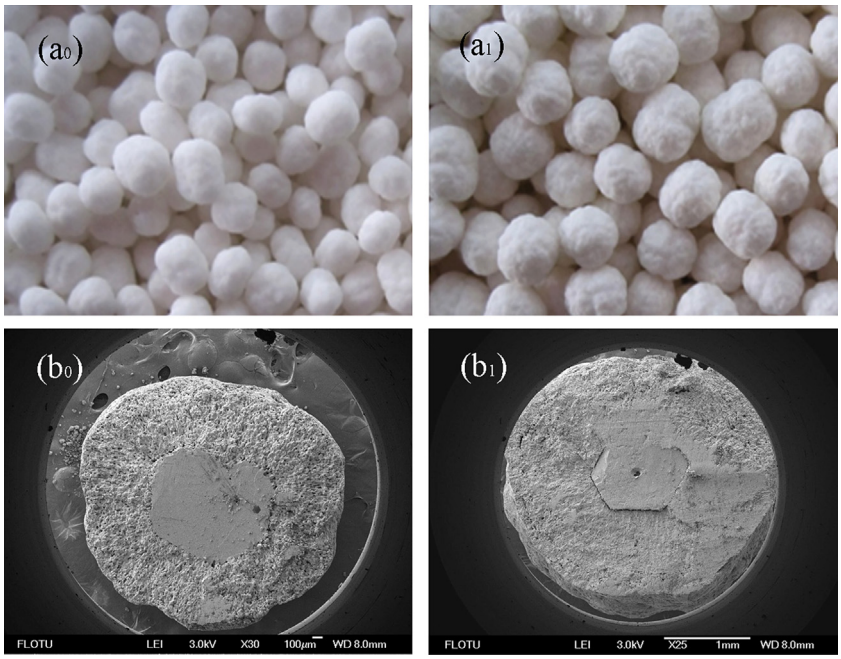

Fig. 3. The produced granules and their cross section structure: (a) granules and (b) cross section of a single granule (subscript 0 for pure $(NH_4)_2SO_4$; 1 for $(NH_4)_2SO_4$ with 5% micro-$CaCO_3$).

difference. Granules obtained with the other additives and with different amounts of additives showed a similar core–shell structure. The crushing strength of most granules was in the range of 20–40 N.

3.2. Coating efficiency

The coating efficiency E depends on the growth rate of the granules, which can be expressed by

$$\frac{dm}{dt} = k_0 - k_1, \quad (2)$$

where k_0 was the spray rate of solute, which was constant in the experiments, and k_1 was the loss rate due to entrainment, including uncollected droplets and attrition losses. In our granulation system, the bed was high enough to give a high collection efficiency; so attrition loss was the main term in k_1. The experimental data showed that the granule mass increased linearly with granulation time, indicating that the loss rate k_1 was almost constant during the granulation process.

When pure $(NH_4)_2SO_4$ solution was used as the feed solution, a large amount of dust was formed, and the coating efficiency was only 58%. However, when $CaCO_3$ or SiO_2 particles were added into the $(NH_4)_2SO_4$ solution, the coating efficiency increased remarkably. The presence of the added particles reduced the entrainment loss rate k_1. Table 3 shows the change in coating efficiency versus additive amount. For each additive, the coating efficiency increased with additive amount. The highest efficiency was 94% when 5% micro-$CaCO_3$ was added.

The effects of the three kinds of additives were compared. Both nano- and micro-$CaCO_3$ additives gave a higher increase in coating efficiency than nano-SiO_2. Adding micro-$CaCO_3$ gave a higher coating efficiency than adding the same amount of nano-$CaCO_3$, especially for 4% and 5% additive amounts. The order of increasing coating efficiency was micro-$CaCO_3$ > nano-$CaCO_3$ > nano-SiO_2 for the same additive amount. For more N content in the product, a lower additive amount is preferable in fertilizer production. Table 3 shows that adding 1% micro-$CaCO_3$ gave 83.5% coating efficiency, indicating micro-$CaCO_3$ is the most promising additive.

3.3. Crushing strength of the product granules

Walker et al. (1997) correlated the crushing strength of a granular NPK (nitrogen, phosphorus, potassium) fertilizer with particle size. Loganathan, Hedley, Clark, and Bolan (1992) found a similar correlation for the strength of granular $(NH_4)_2SO_4$. In this work, the scatter diagrams of granule strength versus diameter were prepared, as shown in Fig. 4 for the granules produced with different amounts of micro-$CaCO_3$. A positive correlation of crushing strength with granule diameter was observed in all the data sets, indicating that the granule diameter has a strong influence on crushing strength. This result is consistent with literature reports (Loganathan et al., 1992; Walker et al., 1997).

In order to quantitatively analyze the strength–diameter relationship, the averaging of 30 neighborhood points was used to filter out random noise. The smoothed strength–diameter curves in Fig. 5 show more obvious linear relationship, and they were fitted by using $y = kx$. The k values, defined as the granule crushing strength coefficients, are listed in Table 4. A larger k value means higher granule crushing strength at the same diameter. Table 4 shows that the granules of the same size produced with additives have higher strength than that of pure $(NH_4)_2SO_4$.

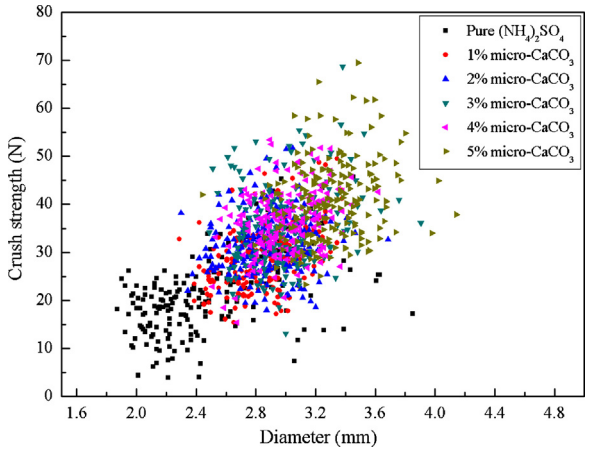

Fig. 4. The strength–diameter scatter diagram of granules with different amounts of micro-$CaCO_3$.

3.4. Effect of additives on granule structure

Fig. 6 shows the SEM images of the surfaces and the inner structures of granules. The structure of pure $(NH_4)_2SO_4$ granule is greatly different from those for granule of $(NH_4)_2SO_4$ with 5% micro-$CaCO_3$. The distinctive feature is that pure $(NH_4)_2SO_4$ granule has a loosely packed sand-like structure while the granules with additives have far more compact structures. The crystallites in pure $(NH_4)_2SO_4$ granule are more isolated than those for $(NH_4)_2SO_4$ granules with additives. Fig. 6 also shows that the structures of $(NH_4)_2SO_4$ granules with 5% nano-SiO_2 or 5% nano-$CaCO_3$ were similar to those with 5% micro-$CaCO_3$.

Fig. 7 shows the SEM images of the granule surface and inner structure obtained with different amounts of additives. Since there is structural similarity for granules obtained with different additives, granules obtained with 1%, 3% and 5% micro-$CaCO_3$ were chosen for study of additive amount effect. As the additive amount increased, the crystallite size decreased and the surface morphology became more uniform. The inner structures were all compact and did not change much.

Mercury porosimetry (Autopore IV 9510, USA) was used for granule porosity characterization. The average pore diameters of granules obtained with 3% of the different additives are listed in Table 5. The pore size distribution curves are shown in Fig. 8. The pure $(NH_4)_2SO_4$ granules had an obviously larger average pore diameter than $(NH_4)_2SO_4$ granules produced with additives, and the pore volume of the pores in the 2000–3000 nm range in the

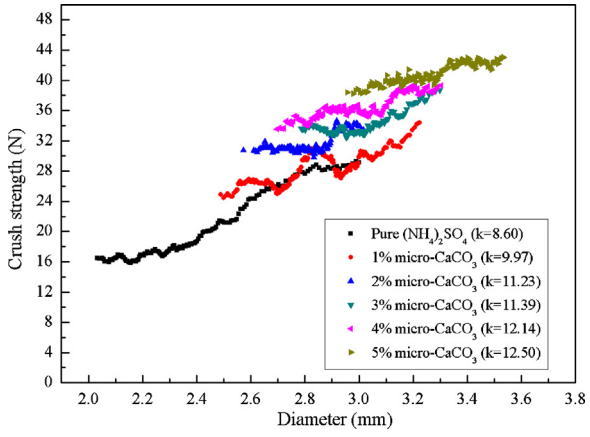

Fig. 5. Filtered curves of granule crushing strength vs. its diameter.

Table 3
Coating efficiency with different additives.

Additive quantity, wt% of $(NH_4)_2SO_4$		0	1	2	3	4	5
Coating efficiency (%)	Nano-SiO_2	57.9	69.1	74.7	75.6	83.3	86.4
	Nano-$CaCO_3$	57.9	82.7	83.3	86.7	87.2	88.5
	Micro-$CaCO_3$	57.9	83.5	83.8	86.9	91.8	94.3

Table 4
Granule crushing strength coefficient *k* for different additives.

Additive quantity, wt% of $(NH_4)_2SO_4$	0	1	2	3	4	5
Nano-SiO_2	8.60	11.73	11.23	10.83	11.56	11.34
Nano-$CaCO_3$	8.60	10.10	11.51	11.64	11.40	12.11
Micro-$CaCO_3$	8.60	9.97	11.23	11.39	12.14	12.50

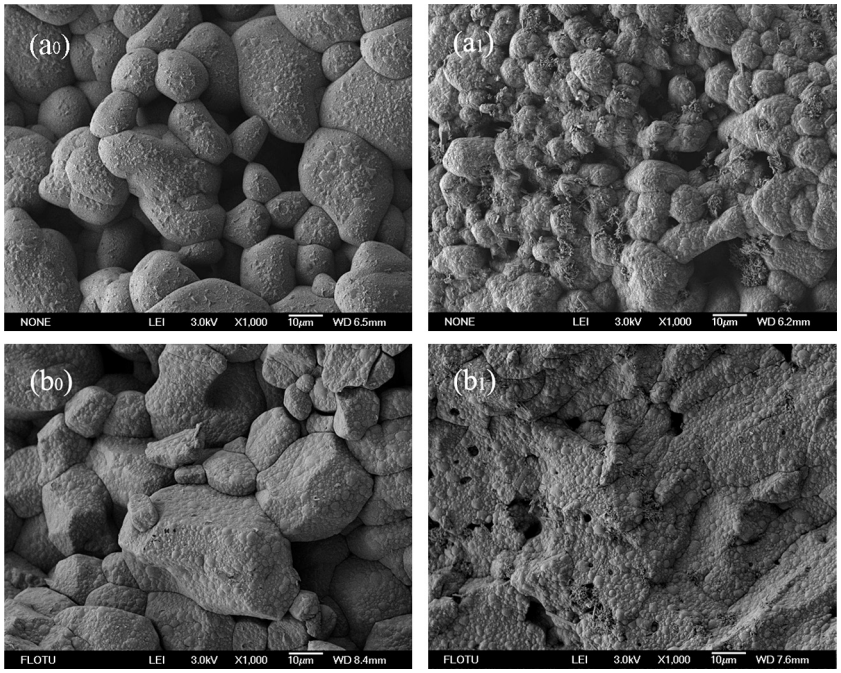

Fig. 6. SEM images of (a) surface and (b) inner structure of the granules. Subscript 0 for pure $(NH_4)_2SO_4$; subscript 1 for $(NH_4)_2SO_4$ with 5% nano-SiO_2; subscript 2 for $(NH_4)_2SO_4$ with 5% nano-$CaCO_3$; subscript 3 for $(NH_4)_2SO_4$ with 5% micro-$CaCO_3$.

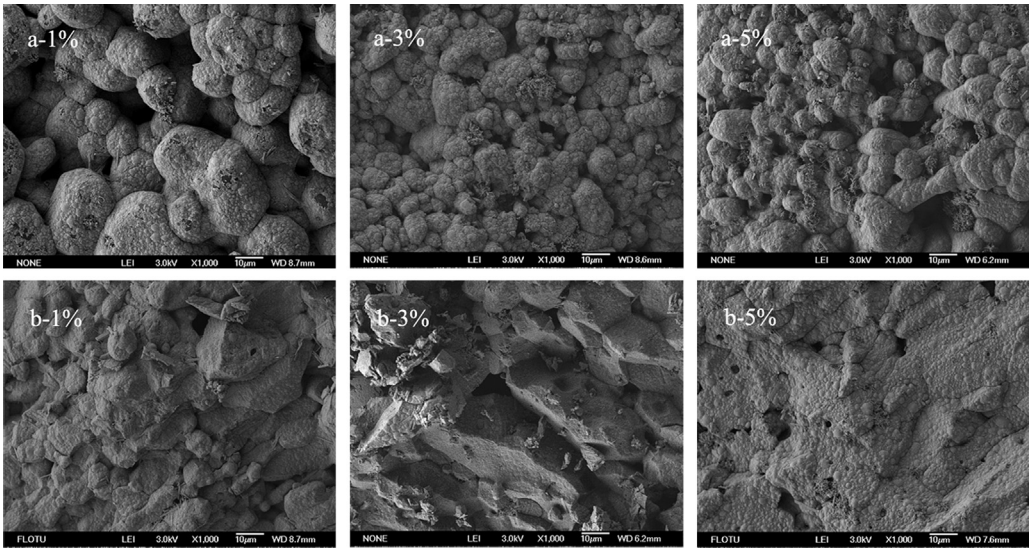

Fig. 7. SEM images of surface (a) and inner structure (b) of the $(NH_4)_2SO_4$ granules with 1%, 3% and 5% micro-$CaCO_3$.

Table 5
Average pore diameter in $(NH_4)_2SO_4$ granules with 3% additive of different kinds.

$(NH_4)_2SO_4$ granules	Pure	Nano-SiO_2	Nano-$CaCO_3$	Micro-$CaCO_3$
Average pore diameter (nm)	364.7	35.8	18.7	51.1

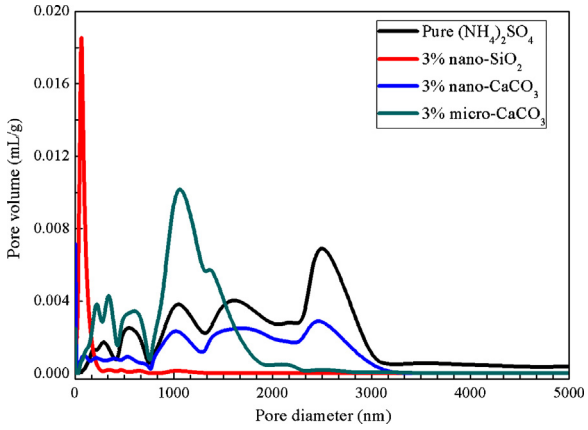

Fig. 8. Pore size distribution of $(NH_4)_2SO_4$ granules with 3% additive of different kinds.

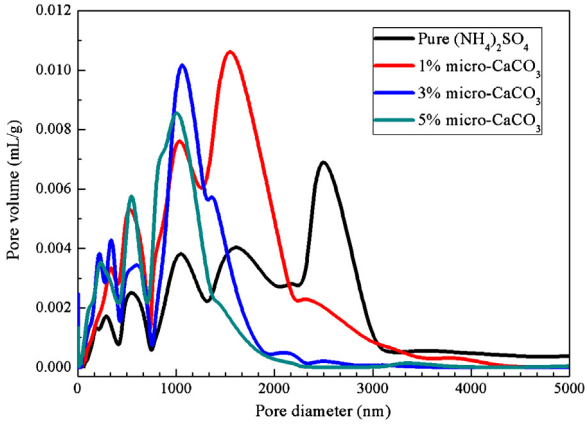

Fig. 9. Pore size distribution of $(NH_4)_2SO_4$ granules with different percentages of micro-$CaCO_3$.

pure $(NH_4)_2SO_4$ granules was much larger. The result indicated that when additives were introduced, the granules had a more uniform structure, which was consistent with the structural features shown in Fig. 6.

The average pore diameters of the $(NH_4)_2SO_4$ granules obtained with different amounts of micro-$CaCO_3$ added are listed in Table 6. The pore volume versus pore size curves are shown in Fig. 9. The average pore diameter decreased with increasing amount of micro-$CaCO_3$ added, that is, the pore size distribution moved toward the smaller pore size. As compared to pure $(NH_4)_2SO_4$, the average pore diameter showed a sharp decrease when only 1% micro-$CaCO_3$ was used, which is consistent with the structural features shown in Figs. 6 and 7.

Table 6
Average pore diameter of $(NH_4)_2SO_4$ granules with different amounts of micro-$CaCO_3$.

$(NH_4)_2SO_4$ granules with micro-$CaCO_3$	0%	1%	3%	5%
Average pore diameter (nm)	364.7	116.2	51.1	45.1

The consistent results obtained for the granule morphology and porosity confirmed that with introduction of additives in the spray coating the structure of the granules obtained became more compact and uniform than that of granules produced with pure $(NH_4)_2SO_4$. It was inferred that the compact structure had a stronger attrition resistance than the sand-like structure of the pure $(NH_4)_2SO_4$ granules, and this resulted in higher coating efficiency. More compact and uniform structure also contributed to a larger crushing strength.

3.5. Effect of additives on $(NH_4)_2SO_4$ crystallization

The above discussion showed that when additive particles were introduced into the spray coating solution, the textural structure of the granules was changed. It was inferred that the additive particles served as heterogeneous nuclei that changed the crystallization of the $(NH_4)_2SO_4$ droplets, thus causing a different structure. Coating granulation is the cumulative outcome of a large quantity of droplets crystallizing onto the core particle surface. As a single droplet moves toward the core particle surface from the nozzle, water evaporates and the $(NH_4)_2SO_4$ concentration in the droplet increases. When the $(NH_4)_2SO_4$ in the droplet reaches a certain supersaturation, primary nuclei begin to form. For a pure $(NH_4)_2SO_4$ droplet, the nuclei are formed by a homogeneous nucleation process, and the primary nuclei are formed spontaneously. For the $(NH_4)_2SO_4$ droplet with SiO_2 or $CaCO_3$ particles in it, the additive particles provide a heterogeneous surface that may induce nucleation at a lower supersaturation, leading to faster crystallization than homogeneous crystallization (Tavare, 1995).

When droplets collide with and adhere to the core particle surface, the pure $(NH_4)_2SO_4$ in the droplet begins to crystallize fast and spontaneously (McCabe, Smith, & Harriott, 2000), thus forming an isolated and loosely packed structure. This is a type of structure that would cause more dust formation by attrition, leading to a low coating efficiency. In contrast, the $(NH_4)_2SO_4$ in the droplet with additive particles would have already crystallized gradually before contact with the core particle surface. So the $(NH_4)_2SO_4$ in the droplet was already partly crystallized when it contacted the granule surface, thus resulting in a more uniform and compact structure. This would give the granule a higher strength and the granulation would have a high coating efficiency. A schematic illustration of the crystallization rate in the single droplet versus time for both homogeneous and heterogeneous processes is shown in Fig. 10. It may be inferred that the heterogeneous nuclei led to a more uniform crystallization, as was verified by the smaller average pore size of the $(NH_4)_2SO_4$ granules with more additives in Table 6.

The crystal structures of the different granules were analyzed using X-ray diffraction (XRD, D8-Advance, Brucker, Germany). Typical patterns for granules of pure $(NH_4)_2SO_4$ and the $(NH_4)_2SO_4$ with micro-$CaCO_3$ additive are shown in Fig. 11. The patterns for $(NH_4)_2SO_4$ granules with nano-SiO_2 and nano-$CaCO_3$ were the same as those for pure $(NH_4)_2SO_4$ and $(NH_4)_2SO_4$ with micro-$CaCO_3$, respectively. The diffraction peaks of $(NH_4)_2SO_4$ were the same in all the samples, except for the peak at $2\theta = 9^\circ$ found in the samples of $(NH_4)_2SO_4$ with nano- and micro-$CaCO_3$ additives. This was confirmed to be the diffraction peak of $(NH_4)_2Ca(SO_4)_2{\cdot}2H_2O$ generated from the reaction between $CaCO_3$ and $(NH_4)_2SO_4$ (Mori,

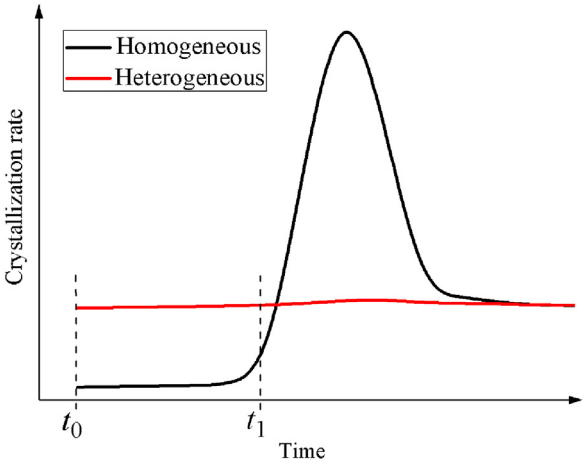

Fig. 10. Sketch of the crystallization process in a single droplet, with t_0 standing for solution atomization and t_1 for contact with the granule surface.

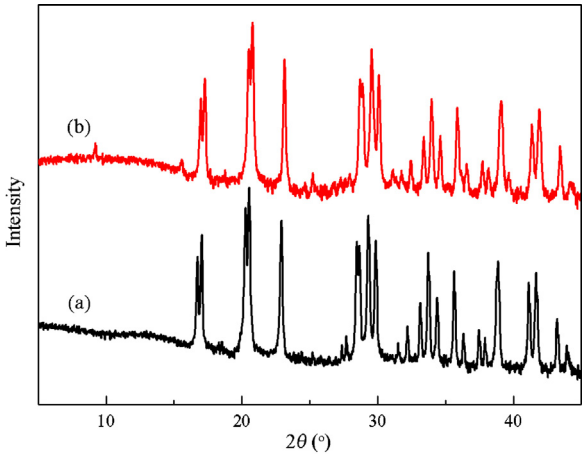

Fig. 11. XRD patterns for different granules: (a) pure $(NH_4)_2SO_4$ and (b) $(NH_4)_2SO_4$ with 5% micro-$CaCO_3$.

Nishikawa, & Iwasaka, 1998):

$$CaCO_3 + 2(NH_4)_2SO_4 + H_2O \rightarrow (NH_4)_2Ca(SO_4)_2{\cdot}2H_2O + 2NH_3 + CO_2 \quad (3)$$

The XRD analysis indicated that the introduction of the additives only changed the crystallization process in terms of its effect on the crystallization rate. The different crystallization processes did not, however, change the crystalline structure of $(NH_4)_2SO_4$.

4. Conclusions

Granulation using pure $(NH_4)_2SO_4$ aqueous solution spray-coated onto $(NH_4)_2SO_4$ grains in a fluidized bed has low coating efficiency. By adding small amounts of small additive particles into the feed solution, the coating efficiency was increased from 58% to over 90%. The effect of different additive particles on increasing coating efficiency was in the order: micro-$CaCO_3$ > nano-$CaCO_3$ > nano-SiO_2. $(NH_4)_2SO_4$ granules of 2–4 mm in size and with a crushing strength range of 20–40 N were obtained by such spray-coating granulation. The granule crushing strength increased with the diameter, and the crushing strength was higher when an additive was used. The additive particles provided a heterogeneous surface that induced $(NH_4)_2SO_4$ nucleation, causing the $(NH_4)_2SO_4$ to crystallize uniformly and form a more compact structure than the case with pure $(NH_4)_2SO_4$ solution. Heterogeneous crystallization enhanced the formation of granules with a compact and uniform structure that increased attrition resistance in the fluidized bed, thus increasing the coating efficiency. More compact structure also resulted in higher granule strength. The introduction of a small amount of additives led to a spray coating granulation process of $(NH_4)_2SO_4$ aqueous solution with higher coating efficiency.

Acknowledgment

The authors wish to express their appreciation for the financial support to this study from the National Natural Science Foundation of China (NSFC No. 20876085).

References

Chien, S. H., Gearhart, M. M., & Villagarcia, S. (2011). Comparison of ammonium sulfate with other nitrogen and sulfur fertilizers in increasing crop production and minimizing environmental impact: A review. *Soil Science*, *176*, 327–335.

Chou, M. M., Bruinius, J. A., Benig, V., Chou, S.-F. J., & Carty, R. H. (2005). Producing ammonium sulfate from flue gas desulfurization by-products. *Energy Sources*, *27*, 1061–1071.

Hagiu, C., Ciupitu, G., & Apostolescu, N. (1998). Research on the process for ammonium sulphate production from phosphogypsum. *Revista de Chimie*, *49*, 241–244 [in Roumain].

Hanna, A. A., & Ahmed, S. M. (1999). Phosphogypsum utilization. Part II. Preparation of ammonium sulphate. *Journal of Materials Science & Technology*, *15*, 571–574.

Hemati, M., Cherif, R., Saleh, K., & Pont, V. (2003). Fluidized bed coating and granulation: Influence of process-related variables and physicochemical properties on the growth kinetics. *Powder Technology*, *130*, 18–34.

Loganathan, P., Hedley, M. J., Clark, S. A., & Bolan, N. S. (1992). Granulation of finely crystalline ammonium sulphate using calcium oxide and sulphuric acid. *Fertilizer Research*, *31*, 85–93.

Löffler, F. (1988). *Staubabscheiden*. Stuttgart: Thieme Verlag.

Martin, S. T., Schlenker, J., Holly, J., & Duckworth, O. W. (2001). Structure–activity relationships of mineral dusts as heterogeneous nuclei for ammonium sulfate crystallization from supersaturated aqueous solutions. *Environmental Science & Technology*, *35*, 1624–1629.

McCabe, W. L., Smith, J. C., & Harriott, P. (2000). *Unit operations of chemical engineering*. New York: McGraw-Hill.

Mori, I., Nishikawa, M., & Iwasaka, Y. (1998). Chemical reaction during the coagulation of ammonium sulphate and mineral particles in the atmosphere. *Science of the Total Environment*, *224*, 87–91.

Oatis, S., Imre, D., McGraw, R., & Xu, J. (1998). Heterogeneous nucleation of a common atmospheric aerosol: Ammonium sulfate. *Geophysical Research Letters*, *25*, 4469–4472.

Onasch, T. B., McGraw, R., & Imre, D. (2000). Temperature-dependent heterogeneous efflorescence of mixed ammonium sulfate/calcium carbonate particles. *The Journal of Physical Chemistry A*, *104*, 10797–10806.

Pant, A., Parsons, M. T., & Bertram, A. K. (2006). Crystallization of aqueous ammonium sulfate particles internally mixed with soot and kaolinite: Crystallization relative humidities and nucleation rates. *The Journal of Physical Chemstry A*, *110*, 8701–8709.

Tavare, N. S. (1995). *Industrial crystallization—Process simulation, analysis and design*. New York: Plenum Press.

Tinge, J. T., Krooshof, G. J. P., Smeets, T. M., Vergossen, F. H. P., Krijgsman, J., Hoving, E., et al. (2007). Direct osmosis membrane process to de-water aqueous caprolactam with concentrated aqueous ammonium sulphate. *Chemical Engineering & Process*, *46*, 505–512.

Uemaki, O., & Mathur, K. B. (1976). Granulation of ammonium sulfate fertilizer in a spouted bed. *Industrial & Engineering Chemistry Process Design and Development*, *15*, 504–508.

Walker, G. M., Magee, T. R. A., Holland, C. R., Ahmad, M. N., Fox, N., & Moffatt, N. A. (1997). Compression testing of granular NPK fertilizers. *Nutrient Cycling in Agroecosystems*, *48*, 231–234.